Inelastic light scattering spectra due to coupled plasmon modes in parallel quantum wires

2001 J. Phys.: Condens. Matter 13 6421

(http://iopscience.iop.org/0953-8984/13/29/311)

INSTITUTE OF PHYSICS PUBLISHING JOURNAL OF PHYSICS: CONDENSED MATTER

J. Phys.: Condens. Matter **13** (2001) 6421–6432 PII: S0953-8984(01)21485-4

Inelastic light scattering spectra due to coupled plasmon modes in parallel quantum wires

Marcos R S Tavares and Guo-Qiang Hai

Instituto de Física de São Carlos, Universidade de São Paulo, 13560-970 São Carlos, SP, Brazil

Received 29 January 2001
Published 6 July 2001
Online at stacks.iop.org/JPhysCM/13/6421

Abstract

The effects of tunnelling on the collective charge-density excitations in two coupled parallel quantum wires and their inelastic light scattering spectra are studied theoretically. The evolution of the collective excitation spectra is presented as a function of the tunnelling strength by altering the symmetry of the two quantum wires. We find that, for two symmetric quantum wires in a resonant tunnelling regime, the plasmon modes are similar to the intrasubband and intersubband plasmon modes. However, in the non-resonant tunnelling condition, the mode mixing occurs. The inelastic light scattering spectrum due to the mixed plasmon modes are discussed in detail.

1. Introduction

Collective excitations and exchange-correlation effects in multisubband quasi-one-dimensional (Q1D) electron gases in both isolated quantum wires [1–11] and multiwire superlattices [4, 12–16] have been extensively studied in the last decade. In particular, the random phase approximation (RPA) has been proved to be a very good approach for describing the plasmon dispersions in such systems [5–7]. In contrast to higher dimensional electron gas systems, the single-particle excitations (SPE) are suppressed in one-dimensional (1D) electron gas due to the energy–momentum conservation leading to a gap in the SPE continuum at low energies [1–4]. In a doubly occupied subband quantum wire, the intrasubband plasmon mode due to the second subband lies in the gap between the two intrasubband SPE continua and is undamped. This feature is essentially different from its counterpart in a two-dimensional system where only one intrasubband plasmon mode is undamped. It has also been shown that the higher frequency intrasubband plasmon mode in the Q1D system (due to the lowest subband) is of an energy proportional to $q|\ln qW|^{1/2}$ at the long wavelength limit, whereas the lower frequency one has a linear q dependence. Here q is the 1D wavevector and W the wire width. Furthermore, a large depolarization shift has been found for the intersubband plasmon mode in single wires. On the other hand, Que *et al* [12] have predicted that, for a multiwire superlattice, only one intrasubband plasmon mode is experimentally observable at long wavelength. This feature is independent of either the number of occupied subbands or the possibility of tunnelling between the wires.

0953-8984/01/296421+12$30.00

In a similar way to coupled two-dimensional electron gases [17], optical and acoustic plasmon modes [12, 18–20] were found in two coupled quantum wires. They are respectively due to the in-phase and out-of-phase charge-density oscillations in the two wires. These modes were also studied in multiwire superlattices [3, 12]. Theoretical work has been done on plasmon dispersions [19, 20], electron–electron correlations [21, 22], Coulomb drag [23], and tunnelling effects in these systems [24, 25]. The RPA results were improved by including correlation effects within the self-consistent scheme of STLS [22]. It has been shown that the correlation strength in each wire increases when the electron density decreases. Moreover, the correlations between electrons in different wires increase as the wires are brought closer together. These correlations affect the collective modes in coupled electron gases and might also be responsible for charge-density-wave instabilities. Correlation induced instabilities in collective modes were predicted in coupled quantum wires with low charge density [26, 27]. Very recently it was shown that a weak resonant tunnelling in coupled wires leads to a finite energy value for the acoustic mode at zero wavevector [19]. It was also found that the dynamic depopulation effect in these wires results in bistability in electron transport [16]. In previous work [28], we found that the acoustic plasmon mode in two asymmetric quantum wires in a very weak non-resonance tunnelling condition presents two gaps at finite q. This acoustic mode splitting indicates a resonant coupling between the acoustic plasmon and the single-particle excitations. Tunnelling effects have provided new devices formed by coupled semiconductor quantum wires [25] and have attracted considerable theoretical interest.

Much insight into the many-body effects in Q1D electron systems is gained from optical experiments. In fact, both plasmon and magnetoplasmon modes in these systems were detected by far-infrared (FIR) absorption spectroscopy [18, 29] and resonant inelastic light (Raman) scattering [30, 31]. Recently, several theoretical studies have been published on the FIR spectrum of Q1D electron gases in coupled quantum wires. Within the RPA, Shahbazyan and Ulloa [24] have investigated the effects of weak interwire tunnelling on the FIR absorption spectrum due to both single-particle and collective excitations in two symmetric parabolic quantum wires under a perpendicular magnetic field. They showed that a weak tunnelling introduces a depolarization shift in the intersubband plasmon frequency as well as additional absorption peaks due to intersubband single-particle excitations. Such a spectrum was found to be very sensitive to magnetic fields. For fields larger than a critical value, the plasmon mode is strongly damped by the SPE. Furthermore, Steinebach *et al* [32] studied the FIR absorption of two coupled quantum wires in the presence of magnetic fields with and without tunnelling. Their FIR absorption spectrum was obtained within the time-dependent Hartree–Fock approximation. The asymmetry between the two wires was considered. They demonstrated that: (i) the acoustic plasmon mode in two asymmetric quantum wires is strongly enhanced; (ii) tunnelling leads to the acoustic magnetoplasmon mode being of higher frequency values than those of the optical ones; and (iii) the acoustic and optical plasmon mode mixing represented by the anticrossing of these plasmon modes in magnetic fields.

Inelastic light scattering is a powerful method for the study of the collective and single-particle excitations in doped semiconductors because the energy and wavevector dispersions can be measured. In fact, the very first 1D signature of the plasmon modes was obtained by resonant inelastic light scattering [30]. The present work is devoted to a theoretical study of the inelastic light scattering spectra in coupled parallel quantum wires with tunnelling. Our results show that a complete plasmon dispersion in this system can be obtained from the calculated Raman spectrum. Our system continuously changes from two coupled quantum wires with tunnelling to a single multisubband wire as the distance between them decreases. We are also able to include an anisotropy in the system to study coupled asymmetric quantum wires. We demonstrate the evolution of the collective excitation spectra in two coupled quantum

wires as a function of the tunnelling strength. The plasmon dispersion and the corresponding inelastic light scattering spectra are obtained through the multisubband dielectric function within the RPA. We show that, in the resonant tunnelling condition, the acoustic mode in the coupled quantum wires evolves to an *intersubband* mode and develops a finite energy at $q = 0$. Moreover, we show that the tunnelling between the wires induces partial damping on the plasmon modes due to different modes mixing.

This paper is organized as follows. The one-particle properties of our system will be briefly discussed in section 2. Theoretical formulation to obtain both the collective charge-density excitation and the inelastic light-scattering spectra will be given in section 3. We present our numerical results and discussions in section 4. We summarize our work in section 5.

2. Two coupled quantum wires with tunnelling

We consider a two-dimensional (2D) system in the xy plane subjected to an additional confinement in the y-direction which forms two quantum wires parallel to each other in the x-direction in which the electrons are free. We assume the 2D system to be ideal, i.e. of zero thickness in the third (z) direction. The confinement potential in the y-direction is taken to be of square well type of height V_b and widths W_1 and W_2 representing the first and the second wire, respectively. The potential barrier between the two wires is of width W_b. The average distance between the parallel 1D electron gases is then given by $d = W_b + (W_1 + W_2)/2$. The subband energies E_n and the wavefunctions $\phi_n(y)$ are obtained from the numerical solution of the one-dimensional Schrödinger equation in the y-direction. We restrict ourselves to the case where $n = 1, 2$ and define $\omega_0 = E_2 - E_1$ as being the gap between two lowest eigenstates. The interpretation of the index n depends on the tunnelling strength between the wires. When there is no tunnelling between them, n should be a wire index. On the contrary, when the wires are in the resonant tunnelling condition, n is interpreted as a subband index. We should point out here the particular case where the two wires are symmetric ($W_1 = W_2$). In the presence of tunnelling in this case, the two lowest wavefunctions are symmetric and antisymmetric functions of y, with $\omega_0 = \Delta_{SAS}$.

We apply the numerical calculation to two coupled quantum wires in a GaAs/$Al_{0.3}Ga_{0.7}As$ structure with $V_b = 228$ meV, the electron effective mass $m^* = 0.07m_e$ (m_e being the free electron mass). By keeping the width of one wire $W_1 = 150$ Å and changing the other W_2, we show in figure 1(a) the probability $P_1^{(n)} = \int_{QW_1} \mathrm{d}y|\phi_n(y)|^2$ of an electron, in the first ($n = 1$) and second subband ($n = 2$), being found in the quantum wire of width W_1 for different barrier widths W_2. The corresponding energy gap between the two subbands is given in figure 1(b). Notice that the two wires are in the resonant tunnelling condition when $W_1 = W_2$. In this situation, $P_1^{(1)} = P_1^{(2)} = 0.5$ which means that electrons in any subband have a 50% chance to be found in both wires. At the same time, the energy difference between the two subbands $\omega_0 = \Delta_{SAS}$ reaches a minimum.

The electron–electron Coulomb interaction $V_{nn'mm'}(q)$ describes two-particle scattering events [28]. In the coupled quantum wires with two occupied subbands ($n, n', m, m' = 1, 2$), it represents the following different physical processes: (i) $V_{1111}(q) = V_A$, $V_{2222}(q) = V_B$, and $V_{1122}(q) = V_{2211}(q) = V_C$, represent the scattering in which the electrons remain in their original subbands (wires); (ii) $V_{1212}(q) = V_{2121}(q) = V_{1221}(q) = V_{2112}(q) = V_D$, represent the scattering in which both electrons change their subband (wire) indices; and (iii) $V_{1112}(q) = V_{1121}(q) = V_{1211}(q) = V_{2111}(q) = V_J$ and $V_{2212}(q) = V_{2221}(q) = V_{1222}(q) = V_{2122}(q) = V_H$, represent the scattering in which only one electron suffers intersubband (interwire) transition. Notice that, when there is no tunnelling, $V_D = V_H = V_J = 0$. It is clear that these terms are responsible for the tunnelling effects on the collective excitations.

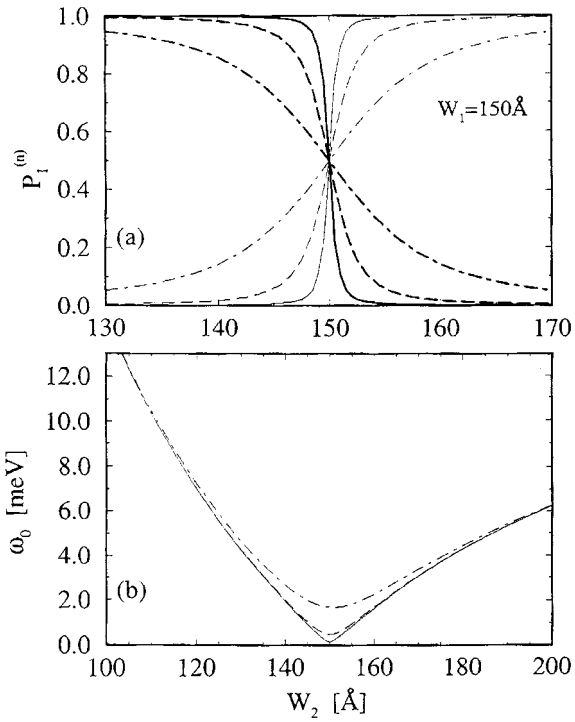

Figure 1. (a) The probability of an electron, in the $n = 1$ (bold full curves) and $n = 2$ (thin full curves) subband, to be found in the quantum wire of $W_1 = 150$ Å as a function of W_2. $W_b = 30$ Å (full curves), 50 Å (broken curves) and 70 Å (dotted–dashed curves); (b) the energy difference ω_0 between the two subbands. $V_b = 228$ meV and $m^* = 0.07m_e$.

3. Theoretical formulation

For a multisubband electron gas system, the collective excitation spectrum can be obtained by the zeros of the determinant of the dielectric matrix [4] $\varepsilon_{nn'mm'}(q,\omega) = \delta_{nm}\delta_{n'm'} - \Pi_{nn'}(q,\omega)V_{nn'mm'}(q)$. Within the RPA, the function $\Pi_{nn'}(q,\omega)$ is the 1D non-interacting irreducible polarizability. In the presence of impurity scattering, we use the formula proposed by Mermin [33] with a phenomenological damping constant γ describing the level broadening.

We restrict ourselves to a two subband model throughout this paper. Thus, using the condition $\det|\varepsilon_{nn'mm'}(q,\omega)| = 0$, the collective charge-density excitation spectrum is determined by the following equation:

$$\begin{aligned}[1 - V_D(\Pi_{12}+\Pi_{21})][(1 - V_A\Pi_{11})(1 - V_B\Pi_{22}) - V_C^2\Pi_{11}\Pi_{22}] \\ +(\Pi_{12}+\Pi_{21})[2V_CV_JV_H\Pi_{11}\Pi_{22} - V_J^2\Pi_{11}(1 - V_B\Pi_{22}) \\ -V_H^2\Pi_{22}(1 - V_A\Pi_{11})] = 0. \end{aligned} \tag{1}$$

The inelastic light scattering intensity of an electron gas is proportional to its dynamical structure factor, or equivalently to the imaginary part of the polarization function [34]. For the present coupled Q1D electron gases, the inelastic light scattering spectrum can be written as

$$I(q_y,q,\omega) = -\sum_{nn'mm'} \mathrm{Im}\,[\chi_{nn'mm'}(q,\omega)A_{nn'mm'}(q_y)] \tag{2}$$

with

$$A_{nn'mm'}(q_y) = \int \mathrm{d}y \int \mathrm{d}y'\, \phi_n(y)\phi_{n'}(y) \exp[-\mathrm{i}q_y(y-y')]\phi_m(y')\phi_{m'}(y')$$

where q_y is related to the wavevector of the incident light and the density–density correlation function $\chi_{nn'mm'}(q,\omega)$ can be obtained by the equation

$$\sum_{ll'} \kappa_{ll',nn'}(q,\omega)\chi_{ll',mm'}(q,\omega) = \delta_{nm}\delta_{n'm'} \tag{3}$$

where

$$\kappa_{nn'mm'} = \delta_{nm}\delta_{n'm'}/\Pi_{nn'} - V_{nn'mm'}(q).$$

One is able to notice that $\mathrm{Re}\,[\chi_{nn'mm'}(q,\omega)] = \mathrm{Re}\,[\chi_{mm'nn'}(q,\omega)]$ and $\mathrm{Im}\,[A_{nn'mm'}(q_y)] + \mathrm{Im}\,[A_{mm'nn'}(q_y)] = 0$. Therefore

$$I(q_y,q,\omega) = -\sum_{nn'mm'} \mathrm{Im}\,[\chi_{nn'mm'}(q,\omega)]\mathrm{Re}\,[A_{nn'mm'}(q_y)]. \tag{4}$$

From the above equations, we see that $\mathrm{Re}\,[A_{nn'mm'}(q_y)]$ is independent of either q or ω, but it could play an important role in the scattering intensity due to each plasmon mode.

4. Numerical results and discussions

As we discussed in section 2, the Coulomb interactions V_D, V_H and V_J vanish in the absence of tunnelling between the wires. As a result, (1) reduces to

$$(1 - V_A\Pi_{11})(1 - V_B\Pi_{22}) - V_C^2\Pi_{11}\Pi_{22} = 0. \tag{5}$$

For the sake of discussion, we denote the remaining Coulomb interactions in (5) as $U_A = V_A = V_B$ and $U_C = V_C$, when the two wires are symmetric ($W_1 = W_2$) and there is no tunnelling between them ($V_b = \infty$). In this way (5) can be rewritten as

$$[1 - U_+(\Pi_{11} + \Pi_{22})][1 - U_-(\Pi_{11} + \Pi_{22})] - U_+U_-(\Pi_{11} - \Pi_{22})^2 = 0 \tag{6}$$

where $U_\pm = (U_A \pm U_C)/2$. Notice that in the absence of tunnelling the two wires are isolated from each other and they might have different electron densities (or Fermi energies). When the two wires are of the same electron density, one has $\Pi_{11} = \Pi_{22} = \Pi_0$. The in-phase and out-of-phase plasmon modes are decoupled and determined by the equation

$$1 - 2U_\pm\Pi_0 = 0.$$

It is clear that the potential U_+ and U_- are related to the in-phase and out-of-phase plasmon modes, respectively. However, when the two wires are of different electron densities, $\Pi_{11} \neq \Pi_{22}$ which leads to the coupling between the two plasmon modes, as indicated in (6).

When the tunnelling is present, one should consider only the subband indices as good quantum numbers. The Coulomb interactions V_D, V_H and V_J become finite in this situation because of the overlap between the different wavefunctions. For two symmetric wires ($W_1 = W_2$), however, the Coulomb potential $V_H = V_J = 0$ due to the symmetry of the electron wavefunctions. In this case, (1) reduces into two decoupled equations

$$[(1 - V_A\Pi_{11})(1 - V_B\Pi_{22}) - V_C^2\Pi_{11}\Pi_{22}] = 0 \tag{7}$$

and

$$[1 - V_D(\Pi_{12} + \Pi_{21})] = 0. \tag{8}$$

The solutions of (7) and (8) give rise to the dispersion of the intra- and inter-subband plasmon modes, respectively. Furthermore, we noticed that, in the weak resonant tunnelling condition

of two symmetric quantum wires, $V_A \simeq V_B \simeq V_C = U_+$ and $V_D \simeq U_-$. In comparison with (6), (7) and (8) can be written as $1 - U_+(\Pi_{11} + \Pi_{22}) = 0$ and $1 - U_-(\Pi_{12} + \Pi_{21}) = 0$, respectively.

Figure 2 shows the plasmon dispersions in two coupled GaAs/$Al_{0.3}Ga_{0.7}$As quantum wires with a barrier of width $W_b = 30$ Å. One quantum wire is of width $W_1 = 150$ Å and the other is of different widths: $W_2 =$ (a) 150 Å; (b) 140 Å; (c) 125 Å; and (d) 110 Å. The total electron density in the system is $N_e = 10^6$ cm^{-1}. In figure 2(a), the two quantum wires are in the resonant tunnelling condition. The energy gap between the two subbands is $\Delta_{SAS} = 1.70$ meV. In this case, the electron densities in the first ($n = 1$) and the second ($n = 2$) subbands are $N_1 = 0.57 \times 10^6$ cm^{-1} and $N_2 = 0.43 \times 10^6$ cm^{-1}, respectively. The shadow areas indicate the SPE which result in the Landau damping on the collective excitation modes. As discussed before, $V_H = V_J = 0$ in this case. It leads to the decoupling between the intra- and inter-subband plasmon modes. Equation (7) gives rise to two intrasubband plasmon modes plotted in thick full curves, which are the so-called in-phase or 'optical' plasmon modes. The high-frequency intrasubband mode (1,1) is mainly due to the first subband while the low-frequency one (2,2) is mainly due to the second subband. The small energy gap Δ_{SAS} between the two subbands leads to a very narrow gap between the two intrasubband SPE continua where the mode (2,2) lies. Equation (8) yields two intersubband plasmon modes indicated in thick broken curves. They correspond to the out-of-phase (or 'acoustic') modes which are of finite energy at $q = 0$ due to the tunnelling effect. It is clear that the Coulomb potential V_D in this case is responsible for the intersubband modes, as indicated in (8). We also see a large depolarization shift of the high-frequency intersubband plasmon mode (1,2). The intersubband single-particle excitation continuum is of a finite frequency ($\omega = \Delta_{SAS}$) at $q = 0$. The occupation of the second subband opens up a gap in this continuum where the low-frequency intersubband mode $(1, 2)'$ shows up.

For $\omega \gg \Delta_{SAS}$, $\Pi_{12} + \Pi_{21} \approx \Pi_{11} + \Pi_{22}$ in (8). Therefore, it is not difficult to understand that at high frequencies the intersubband plasmon mode (1,2) approaches the acoustic mode in coupled wires without tunnelling. Notice that, due to the symmetry of the confinement potential, intra- and intersubband modes do not couple to each other in such a way that: (i) the intrasubband plasmon modes cross over the intersubband modes; and (ii) the intersubband (intrasubband) single-particle excitations do not damp the intrasubband (intersubband) plasmon modes. As we will discuss later, this feature becomes clearer in the inelastic light scattering spectrum.

Figure 2(b) shows that a mixing between the intra- and inter-subband plasmon modes occurs when the two quantum wires become asymmetric. Notice that, by decreasing the second wire width W_2 to 140 Å, the energy gap between the two subbands increases. So, the intersubband modes shift to higher frequencies at small q, while the depolarization shift in the mode (1,2) decreases. The latter results from the decrease of the electron density of the second subband. The open circles indicate the peak position in the inelastic light scattering spectra which will be discussed later. We need to mention that in this case one cannot obtain a complete plasmon spectrum from the zeros of the determinant of the dielectric matrix because of the effects of the mode mixing through tunnelling. We found that the high-frequency intrasubband mode (1,1) is strongly mixed with the high-frequency intersubband mode (1,2). Moreover, there is a coupling between the low-frequency intrasubband mode (2,2) and the intersubband mode $(1, 2)'$. Notice that there is an anticrossing between these plasmon modes.

When we further reduce W_2 to 125 Å, the intersubband plasmon mode (1,2) is totally located above the intrasubband mode (1,1), as we show in figure 2(c). In this case, no root of (1) was found for the low-frequency intrasubband mode. But we can observe this mode in the light scattering spectra as indicated by the open circles. When $W_2 = 110$ Å (figure 2(d)),

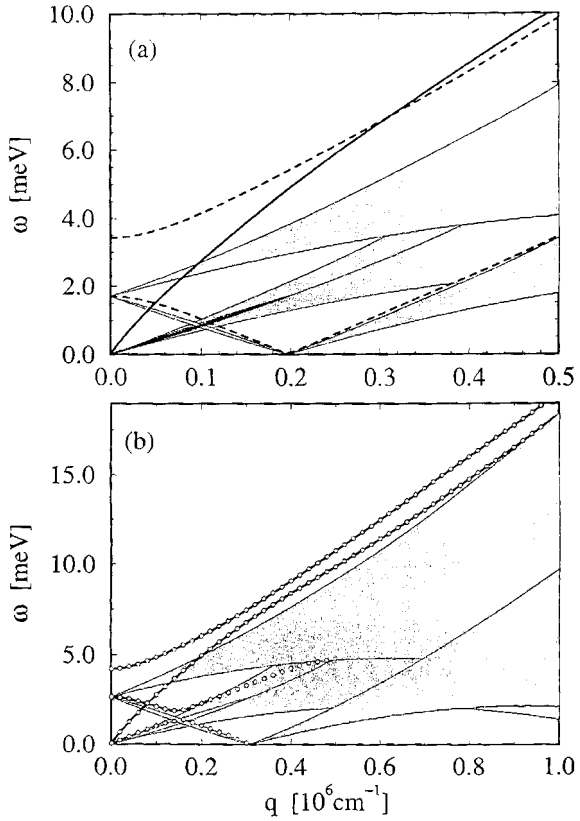

Figure 2. Plasmon dispersions in two coupled GaAs/$Al_{0.3}Ga_{0.7}As$ ($V_b = 228$ meV) quantum wires separated by a barrier of width $W_b = 30$ Å with $W_1 = 150$ Å and $W_2 =$ (a) 150 Å; (b) 140 Å; (c) 125 Å; and (d) 110 Å. The total electron density is $N_e = 10^6$ cm^{-1}. In (a) the full (broken) curves indicate the intrasubband (intersubband) plasmon modes. The high- and low-frequency intrasubband (intersubband) modes are called (1,1) and (2,2) ((1,2) and $(1, 2)'$), respectively. The open circles in (b) and (c) indicate the peak position in the Raman spectra. The shadow area presents the single-particle excitation continua.

the tunnelling becomes very weak due to the asymmetry in the two wires. This situation is similar to that without tunnelling between the wires. Figure 2(d) shows that there are only two small branches characterizing the intersubband plasmon modes at small q. But now we observe two intrasubband modes. They are actually from two different quantum wires with Coulomb coupling.

From the above discussion, we verified that the zeros of det $|\varepsilon_{nn'mm'}(q, \omega)|$ were not able to provide the complete information about the plasmon modes in the two coupled quantum wires. In order to access a complete spectrum of the collective excitation and the relative importance of the different plasmon modes, one should calculate the inelastic light scattering spectrum of the electron gas in the range of the plasmon frequency.

Figure 3(a) shows the inelastic light scattering (Raman) spectra due to the plasmon modes given in figure 2(a). Here the phenomenological damping constant is taken as $\gamma = 0.05$ meV. The broken and full curves correspond to $q_y d = 0$ and $\pi/2$, respectively, where d is the average distance between the two quantum wires. For $q_y d = 0$ (broken curves), there is no coupling between the incident light and the *intersubband* plasmon modes because the

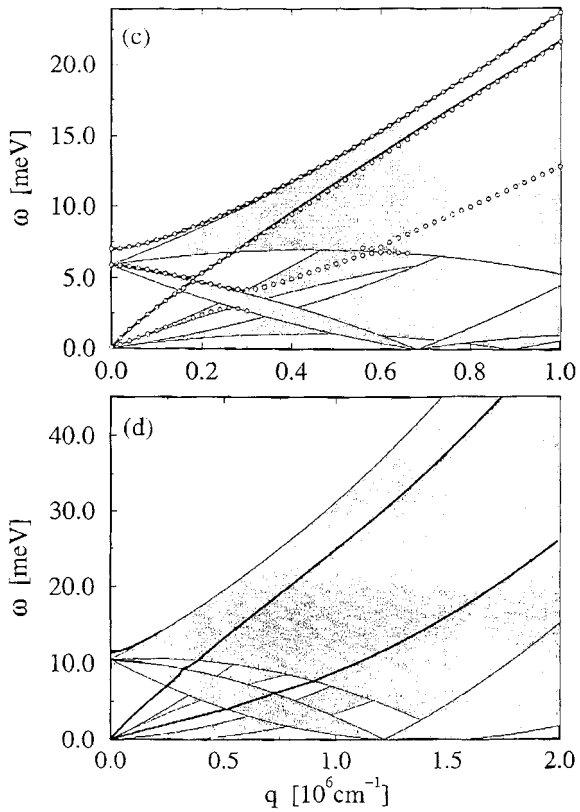

Figure 2. (Continued)

corresponding matrix element $\mathrm{Re}\,[A_{nn'mm'}(q_y)]$ vanishes. This means that the intersubband plasmon modes do not scatter the incident light of long wavelength. One only can observe the intrasubband plasmon mode scattering in the Raman spectrum at $q_y \to 0$, as we show in figure 3(a). As discussed in the previous section, we also cannot identify the scattering peaks due to the low-frequency intrasubband plasmon mode (2,2) because of its weakness. For $q_y d = \pi/2$, the spectra (the full curves) exhibit two main scattering peaks due to the high-frequency intrasubband mode (1,1) and intersubband plasmon mode (1,2). At $q = 0$, the scattering intensity due to the intrasubband mode is zero, but that due to the intersubband mode is finite. The former (latter) increases rapidly (slowly) as the wavevector q increases. They cross over at about $q = 0.3 \times 10^6$ cm^{-1}. We also find a small contribution coming from the mode $(1, 2)'$. The existence of this collective mode is a particular feature of the Q1D system. Our results show that, for two strongly coupled identical quantum wires with two occupied subbands, the plasmon dispersions and their relative spectral weights are very similar to those in the single quantum wire.

The plasmon mode mixing in two coupled asymmetric quantum wires leads to interesting effects in the inelastic light scattering spectrum. The corresponding Raman spectra of figure 2(b) is shown in figure 3(b). The open circles in figure 2(b) indicate the peak position in the Raman spectra with a very small broadening constant $\gamma = 10^{-3}$ meV. Even for $\gamma = 0.05$ meV (as shown in figure 3(b)) we are still able to clearly observe four peaks in the full curves for $q = 0.05$ and 0.1×10^6 cm^{-1}. These peaks correspond to the four plasmon

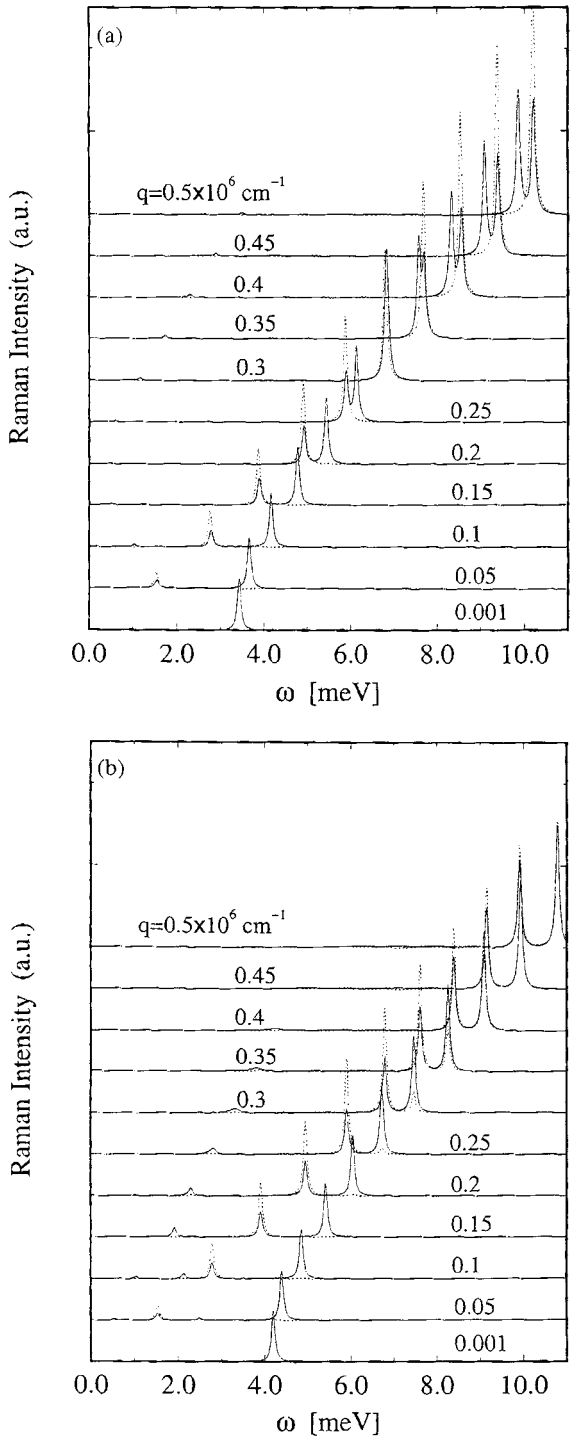

Figure 3. The inelastic light scattering spectra at different q in the coupled quantum wires corresponding to figure 2 with $\gamma = 0.05$ meV and $q_y d = 0$ (broken curves) and $\pi/2$ (full curves). The different curves are offset for clarity. The intensity in (d) is reduced by a factor of two as compared with the others.

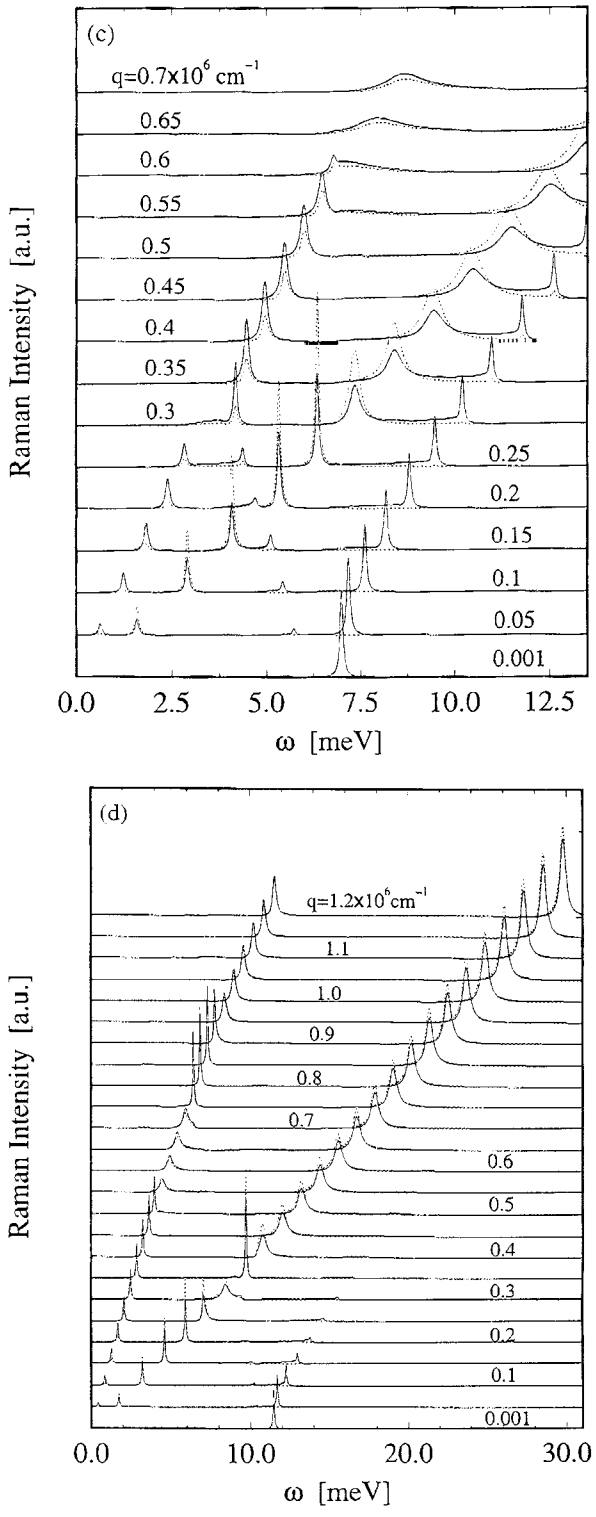

Figure 3. (Continued)

modes in figure 2(b). We also see the anticrossing between the inter- and intra-subband modes at large q. If we compare the broken curves in figures 3(b) and 3(a), we see the extra peak in figure 3(b) due to the mode mixing. Notice that the weight of the lower frequency peak transfers to the higher frequency one as q increases.

The electron density in the second subband decreases as W_2 further decreases. As a result, we can see in figure 3(c) that the intersubband modes lose their spectral weight at large q. However, the mode mixing gets stronger in this case. We also find a scattering peak at the low-frequency side which was absent in the zeros of the determinant of the dielectric matrix (see figure 2(c)). This peak is located in the region of the SPE continuum but it is only partially Landau damped. This kind of damping can be observed clearly when the modes get into the SPE continuum (by comparing figures 2(c) and 3(c)). Notice that, when the intrasubband plasmon mode (1,1) lies in the intersubband SPE continuum for $q > 0.28 \times 10^6$ cm^{-1}, there is only a partial damping on it. Its corresponding scattering peak in figure 3(c) becomes lower and broader. Figure 3(d) shows the inelastic-light scattering spectrum corresponding to figure 2(d). In this case, the intersubband plasmon modes become irrelevant at large q. We also observe a partial Landau damping on the two intrasubband plasmon modes when they enter the intersubband SPE continua.

When we further increase the barrier width, for example $W_b = 70$ Å and take $W_1 = W_2 = 150$ Å, we find $\Delta_{SAS} = 0.14$ meV which indicates a very weak tunnelling between the two quantum wires. Furthermore, if we keep the width of one wire, a very small change in the other leads to the localization of the subband wavefunction in a certain wire as can be seen in figure 1 (the full curves). In this asymmetric case, the acoustic mode splits when its frequency is close to the frequencies of the intersubband-like single-particle excitations. As discussed in our previous work [28], the interactions V_J and V_H are responsible for such a splitting. They represent the electron–electron scattering during which only one of the electrons experiences intersubband transition. When the momentum and energy transfer between these two electrons occurs in the region of the single-particle excitations, there will be a creation of an intersubband electron–hole pair. The momentum and energy conservation in the scattering ensures that such a transition removes the Landau damping. In this sense, the splitting of the acoustic plasmon mode presented in [28] is essentially different from the plasmon mode mixing discussed here.

5. Conclusions

We have studied the collective charge-density excitations and the inelastic light scattering spectra in coupled quantum wires with tunnelling. We showed that, in the resonant tunnelling condition, intrasubband plasmon modes in the symmetric system do not couple to the intersubband plasmon modes. The high-frequency intrasubband mode, carrying most oscillator strength, corresponds to the so-called optical plasmon mode. The intersubband mode, corresponding to the acoustic mode, is of finite frequency at $q = 0$. Moreover, the intersubband plasmon modes do not couple to the long-wavelength incident light and, consequently, it cannot be observed in the Raman scattering for $q_y \to 0$.

For two quantum wires in non-resonant tunnelling, the mode mixing occurs between the different plasmon modes. Such a mixing can be observed by the anticrossing in the plasmon dispersions. This might also be seen from the intensity of the inelastic light-scattering since it leads to a transfer of the oscillator strength from one plasmon mode to the other. On the other hand, the intrasubband-like plasmon mode can be partially Landau damped in the intersubband single-particle excitation continuum. In this case, the often used theoretical approach based on the zeros of the determinant of the dielectric matrix cannot provide a complete dispersion relation of the plasmon modes.

Acknowledgment

This work is supported by Brazilian agencies FAPESP and CNPq.

References

[1] Friesen W I and Bergersen B 1980 *J. Phys. C: Solid State Phys.* **13** 6627
[2] Gold A and Ghazali A 1990 *Phys. Rev.* B **41** 7626
[3] Li Q P and Das Sarma S 1991 *Phys. Rev.* B **43** 11 768
[4] Das Sarma S and Lai W Y 1985 *Phys. Rev.* B **32** 1401
Lai W Y, Kobayashi A and Das Sarma S 1986 *Phys. Rev.* B **34** 7380
[5] Yu-Kuang Hu B and Das Sarma S 1993 *Phys. Rev.* B **48** 5469
[6] Hu G Y and O'Connell R F 1991 *Phys. Rev.* B **44** 3140
Hai G Q, Peeters F M, Devreese J T and Wendler L 1993 *Phys. Rev.* B **48** 12 016
[7] Hwang E H and Das Sarma S 1994 *Phys. Rev.* B **50** 17 267
[8] Wang L and Bishop A R 1995 *Phys. Rev.* B **51** 7407
[9] Sassetti M, Napoli F and Bramer B 1999 *Phys. Rev.* B **59** 7297
Brataas A, Mal'shukov A G, Steinebach C, Gudmundsson V and Chao K A 1997 *Phys. Rev.* B **55** 13 161
[10] Agosti D, Pederiva F, Lipparini E and Takayanagi K 1998 *Phys. Rev.* **57** 14 869
[11] Machado P C M, Leite J R, Osório F A P and Borges A N 1997 *Phys. Rev.* B **56** 4128
[12] Que W 1991 *Phys. Rev.* B **43** 7127
Que W and Kirczenow G 1988 *Phys. Rev.* **37** 7153
Li Q and Das Sarma S 1990 *Phys. Rev.* B **41** 10 268
[13] Yu J X and Xia J B 1996 *Solid State Commun.* **98** 227
Lu X L, Cui H L and Horing N J M 1996 *Solid State Commun.* **77** 331
[14] Latgé A and d'Albuquerque e Castro J 1993 *Phys. Rev.* B **47** 4798
[15] Gold A 1992 *Z. Phys.* B **89** 213
[16] Messica A, Meirav U, Shtrikman H, Umansky V and Mahalu D 1996 *Phys. Rev.* B **54** R5247
[17] Cordes J G and Das A K 1997 *Superlatt. Microstruct.* **25** 1954
Kainth D S, Richards D, Hughes H P, Simmons M Y and Ritchie D A 1998 *Phys. Rev.* B **57** R2065
Das Sarma S and Hwang E H 1998 *Phys. Rev. Lett.* **81** 4216
[18] Demel T, Heitmann D, Grambow P and Ploog K 1988 *Phys. Rev.* B **38** 12 732
Demel T, Heitmann D, Grambow P and Ploog K 1991 *Phys. Rev. Lett.* **66** 2657
[19] Das Sarma S and Hwang E H 1999 *Phys. Rev.* B **59** 10 730
[20] Shikin V, Demel T and Heitmann D 1992 *Phys. Rev.* B **46** 3971
[21] Thakur J S and Neilson D 1997 *Phys. Rev.* B **59** 4671
[22] Mutluay N and Tanatar B 1997 *Phys. Rev.* B **55** 6697
Mutluay N and Tanatar B 1997 *J. Phys.: Condens. Matter* **9** 3033
Gold A and Calmels L 1998 *Phys. Rev.* B **58** 3497
[23] Tanatar B 1996 *Solid State Commun.* **99** 1
[24] Shahbazyan T V and Ulloa S E 1996 *Phys. Rev.* B **54** 16 749
[25] Eugster C and del Alamo J A 1992 *Appl. Phys. Lett.* **60** 642
Bertoni A *et al* 2000 *Phys. Rev. Lett.* **84** 5912
[26] Gold A 1992 *Philos. Mag. Lett.* **66** 163
[27] Wu Z and Ruden P P 1993 *J. Appl. Phys.* **74** 6234
Wu Z and Ruden P P 1992 *J. Appl. Phys.* **71** 1318
Wang R and Ruden P P 1995 *Phys. Rev.* B **52** 7826
[28] Hai G-Q and Tavares M R S 2000 *Phys. Rev.* B **61** 1704
[29] Schuller C, Biese G, Keller K, Steinebach C and Heitmann D 1996 *Phys. Rev.* B **54** R17 304
[30] Goñi A R, Pinczuk A, Winer J S, Calleja J M, Dennis B S, Pfeiffer L N and West K W 1991 *Phys. Rev. Lett.* **67** 3298
[31] Egeler T, Abstreiter G, Weimann G, Demel T, Heitmann D, Grambow P and Schlapp W 1990 *Phys. Rev. Lett.* **65** 1804
[32] Steinebach C, Heitmann D and Gudmundsson V 1997 *Phys. Rev.* B **56** 6742
Steinebach C, Heitmann D and Gudmundsson V 1997 *Phys. Rev.* B **58** 13 944
[33] Mermin N D 1970 *Phys. Rev.* B **1** 2362
[34] Hai G-Q, Studart N and Marques G E 1998 *Phys. Rev.* B **57** 2276